J. Cell. Mol. Med. Vol 12, No 3, 2008 pp. 1049-1060

Functional effects of caloxin 1c2, a novel engineered selective inhibitor of plasma membrane Ca^{2+}-pump isoform 4, on coronary artery

Jyoti Pande [b], Magdalena M. Szewczyk [b], Iwona Kuszczak [a], Shawn Grover [c], E. Escher [d], Ashok K. Grover [a, b, *]

[a] *Department of Medicine, McMaster University, Hamilton, ON, Canada*
[b] *Department of Biology, McMaster University, Hamilton, ON, Canada*
[c] *Math Faculty, University of Waterloo, Waterloo, ON, Canada*
[d] *Department of Pharmacology, Faculty of Medicine and Health Sciences, Université de Sherbrooke, Sherbrooke, QC, Canada*

Received: July 17, 2007; Accepted: October 9, 2007

Abstract

Coronary artery smooth muscle expresses the plasma membrane Ca^{2+} pump (PMCA) isoforms PMCA4 and PMCA1. We previously reported the peptide inhibitor caloxin 1b1 that was obtained by using extracellular domain 1 of PMCA4 as the target (*Am J Physiol Cell*. 290 [2006] C1341). To engineer inhibitors with greater affinity and isoform selectivity, we have now created a phage display library of caloxin 1b1-like peptides. We screened this library by affinity chromatography with PMCA from erythrocyte ghosts that contain mainly PMCA4 to obtain caloxin 1c2. Key properties of caloxin 1c2 are (a) Ki = 2.3 ± 0.3 μM which corresponds to a 20× higher affinity for PMCA4 than that of caloxin 1b1 and (b) it is selective for PMCA4 since it has greater than 10-fold affinity for PMCA4 than for PMCA1, 2 or 3. It had the following functional effects on coronary artery smooth muscle: (a) it increased basal tone of the de-endothelialized arteries; the increase being similar at 10, 20 or 50 μM, and (b) it enhanced the increase in the force of contraction at 0.05 but not at 1.6 mM extracellular Ca^{2+} when Ca^{2+} extrusion *via* the Na^{+}–Ca^{2+} exchanger and the sarco/endoplasmic reticulum Ca^{2+} pump were inhibited. We conclude that PMCA4 is pivotal to Ca^{2+} extrusion in coronary artery smooth muscle. We anticipate caloxin 1c2 to aid in understanding the role of PMCA4 in signal transduction and homeostasis due to its isoform selectivity and ability to act when added extracellularly.

Keywords: calcium pumps • duodenum • plasma membrane • vascular • sperm motility

Introduction

Cellular Ca^{2+} dynamics are pivotal to cell survival and signal transduction. Upon cell stimulation, an increase in cytoplasmic [Ca^{2+}] (Ca^{2+}i) occurs by Ca^{2+} entry *via* various types of channels or Na^{+}–Ca^{2+} exchangers (NCX), and by Ca^{2+} release from sarco/endoplasmic reticulum [1–11]. A decrease in Ca^{2+}i to resting levels then follows. Most mammalian cells express sarco/endoplasmic reticulum Ca^{2+} pumps (SERCA) that sequester Ca^{2+} into the lumen of the sarco/endoplasmic reticulum. NCX may also expel cytosolic Ca^{2+} but with a lower affinity. The

*Correspondence to: Dr. A.K. GROVER,
Department of Medicine, HSC 4N41, McMaster University,
1200 Main Street West,
Hamilton, Ontario L8N 3Z5 Canada.
Tel.: 905-525-9140 x22238
Fax: 905-522-3114
E-mail: groverak@mcmaster.ca

doi: 10.1111/j.1582-4934.2007.00140.x

plasma membrane (PM) contains Ca^{2+} pumps (PMCA) that extrude Ca^{2+} from cells with high affinity. The three systems are expressed at different levels in various tissues and are also regulated by diverse mechanisms.

Defects in PMCA have been associated with various diseases [5,12–15]. PMCA are encoded by four genes (PMCA1–4), whose transcripts may be spliced alternatively to produce proteins that differ in their regulation by calmodulin and protein kinases [9,16–25]. PMCA4 and PMCA1 are expressed in more cell types than are PMCA2 and 3. Various tissues may express the four genes at different levels, *e.g.* human erythrocyte ghosts express mostly PMCA4, coronary artery endothelium expresses mostly PMCA1 and coronary artery smooth muscle expresses both PMCA4 and PMCA1 [9, 26]. PMCA4 is the predominant isoform expressed in all layers of corneal epithelium, except along the basal cell membranes adjacent to the stroma [25, 27]. PMCA isoform distribution changes during development in the CA1 region of hippocampus and it may also alter in disease [28].

Various functions have been attributed to PMCA in different studies. In one strain of transgenic mice, the loss of PMCA4 led to impairment of phasic contractions and caused apoptosis in the portal vein smooth muscle *in vitro* and changes in contractility of bladder smooth muscle [7, 29–34]. Contrary to initial expectations, mice overexpressing PMCA4b under the control of a smooth muscle actin promoter show enhanced contractility [35, 36]. It was suggested that PMCA4b is co-localized with the neuronal NO synthase in the caveoli and an increase in PMCA activity decreases NO production, thereby enhancing contractility. An anchoring role has also been proposed for PMCA4 [37]. PMCA in large part was co-localized in caveolae in cardiac myocytes of transgenic mice overexpressing PMCA4 [38]. Others have reported PMCA to be present in caveolae but did not indicate which isoform [27, 39, 40]. In synaptosomes from pig cerebellum, PMCA4 was associated with cholesterol/sphingomyelin-rich detergent insoluble membrane domains (rafts) but the other PMCA isoforms were in the detergent soluble fractions [27, 39–41]. Changes in caveolar distribution may also alter the role of PMCA in disease process [25–27]. Thus, transgenic mice have proved somewhat useful in deciphering the roles of PMCA isoforms but the animals appear to adapt. Hence, the exact roles of PMCA isoforms in cell function have not been delineated. An availability of PMCA4 selective inhibitors would aid in discerning the roles of PMCA isoforms.

We had previously obtained caloxin 1b1 by screening a random peptide phage display library using partial extracellular domain 1 as a synthetic target followed by affinity chromatography on immobilised PMCA from human erythrocyte ghosts [42]. Here, we report on optimized mutagenesis to create a phage display library of caloxin 1b1-like peptides and its screening to obtain a peptide selective for PMCA4 over PMCA1, 2 and 3.

Materials and methods

Membrane isolation

The protocols for the use of human blood and animal material were approved by the ethics committees of McMaster University. Leaky erythrocyte ghosts were prepared from human, pig and rabbit described previously [43, 44]. In this procedure the leaky ghosts are washed thoroughly with EDTA ((ethylenedinitrilo(-tetraacetic acid) to remove any bound calmodulin, and then aliquots are stored at –80°C in a buffer containing in mM: 130 KCl, 20 HEPES, 0.5 $MgCl_2$, 0.05 $CaCl_2$ and 2 dithiothreitol at pH 7.4. Membrane fraction enriched in the PM was obtained from rabbit duodenal mucosa as described for other tissues [45]. This membrane is rich in PMCA1 and contains very little PMCA4 (unpublished results). Microsomes from SF9 insect cells infected with bacculoviral vectors expressing PMCA2 and PMCA3 were prepared by a previously published method [18].

Construction of phage display library of caloxin 1b1-like peptides

The caloxin 1b1 sequence is encoded by the bolded DNA sequence in the plus strand of the phage display vector M13 KE (New England Biolabs Burlington, Canada): CATGCCCGGGTACCTTTCTATTCTCACTCT**ACTGCTTGGAGTGAGGTTTTGCATCTTTTGTCGAGG**GGTGGAGGTTCGGCCGAAACATG. For random mutagenesis, only the bolded sequence was altered. We retained at each location 91% of the original base and to replace the remainder with 3% of each of the other three bases. This base composition was determined to be optimum to maximize the proportion of peptides with 1, 2 or 3 amino acid

changes. The probability computations were carried out using a Macro written in Excel (Microsoft), which also considered codon degeneracy. We used the following oligonucleotide mixture synthesized by the W. M. Keck Foundation (New Haven, USA):

CATGTTTCGGCCGAACCTCCACC**77876575-555658675555778757877556756 8**AGAGTGAGAATAGAAAGGTACCCGGGCATG, where 5 = 91% A (and 3% each of the other three bases), 6 = 91% G, 7 = 91% C and 8 = 91% T. We used this mixture to construct a library in the M13 KE vector following instructions from the New England Biolabs. Library grade XL Blue II *E. coli* cells were transfected with the resulting library (Stratagene, La Jolla, USA). Phage of the specified individual clones was amplified and used to isolate plasmid DNA, which was sequenced at the MOBIX facility at McMaster University, using a reverse primer 96 bp downstream of the random library site (New England Biolabs).

Screening phage for binding to purified PMCA protein

A bed volume of 200-μl agarose-calmodulin resin (Sigma-Aldrich, USA) was packed into a column (BioRad, USA) and equilibrated with the wash buffer (0.4% Triton X-100, 0.05% phosphatidyl serine and phosphatidyl choline and the following in mM at pH 7.4: 130 KCl, 20 HEPES, 1 $MgCl_2$, 2 dithiothreitol, 0.1 $CaCl_2$). PMCA protein was solubilized from human erythrocyte ghosts, reconstituted with phospholipids, applied on this column, and unbound PMCA removed as described previously [42]. The caloxin 1b1-like phage library was diluted in the wash buffer and mixed with the bound PMCA on a rocker for 60 min. The unbound phage was removed as flow through in four additional washes each with 1.6 ml of wash buffer. PMCA and the bound phage were eluted using a Ca^{2+} free elution buffer, which contained 5 mM EGTA instead of 0.1 mM $CaCl_2$. The eluted phage was acidified with glycine-HCl pH 2.4 on ice for 10 min to dissociate the phage from PMCA, neutralized with Tris-HCl pH 8.0 and then precipitated with polyethyleneglycol-NaCl. This phage was used in the next cycle of the affinity chromatography.

Biochemical assays

The peptides to be tested as inhibitors were synthesized, purified >95% by HPLC and characterized by mass spectrometry by Dalton Pharma Services (Toronto, Canada). The Ca^{2+}–Mg^{2+} ATPase assays were performed by monitoring the disappearance of NADH with fluorescence or absorbance at 37°C in a coupled enzyme assay described earlier [42]. Typically basal Mg^{2+} ATPase was first determined in a 135 μl solution containing 0.2–0.4 mg human erythrocyte ghost protein, 0.1 mM ouabain, 100 mM NaCl, 20 mM KCl, 6 mM $MgCl_2$, 30 mM imidazole-HCl pH 7.0, 0.5 mM EDTA, 0.6 mM NADH, 1 mM pyruvate enol phosphate, excess pyruvate kinase-lactate dehydrogenase, 0.5 mM ATP, 0.5 mM EGTA and 4 μg/ml calmodulin. Then 10 μl of 8 mM $CaCl_2$ was added and the total ATPase activity was determined. The difference between the total ATPase and the basal Mg^{2+} ATPase was the Ca^{2+}–Mg^{2+} ATPase activity. Since light at 340 nm used for monitoring the reaction may cross-link the benzoyl phenylalanine (Bpa) derivatives of caloxin 1c2 to proteins, the Ca^{2+}-Mg^{2+}-ATPase assays using these compounds were performed by following the hydrolysis of [^{33}P]-γ-ATP by modification of a procedure previously described [46–48]. In this procedure, Ca^{2+}–Mg^{2+} ATPase is examined as hydrolysis of [^{33}P]-γ-ATP by determining the amount of [^{33}P]-inorganic phosphate formed by molybdate complex formation and phase partitioning. We considered the possibility that the peptide inhibitors may interfere in steps following the ATP hydrolysis. Therefore, after the hydrolysis step additional peptide was added to attain the same level in all the samples. Caloxin 1c2 and its derivatives, caloxin 1b1 and the random peptide RP1b1 were all dissolved at 25 mM in 10 % ethanol and stored as aliquots at –80°C. The samples were diluted further without ethanol. Final ethanol concentration was the same in the samples.

Contractility studies

Pig hearts were obtained from Maple Leaf Pork, Burlington, ON, Canada. Coronary arteries were dissected, de-endothelialized, cut into 3 mm wide rings and used for contractility studies in organ baths containing Krebs' solution (in mM NaCl 115.5; KCl 4.6; $MgSO_4$ 1.2; NaH_2PO_4 1.2; $CaCl_2$ 2.5; $NaHCO_3$ 22.0; D-glucose 11.1) bubbled with 95% oxygen and 5% carbon dioxide as described previously [49]. The rings under 3 g tension were contracted 2× with 60 mM KCl added to the Krebs' solution before use in any experiments. In one set of experiments the effect of caloxin 1c2 on basal tone was examined in normal Krebs' solution containing 100-μM L-nitroarginyl-methyl ester (L-NAME). In another set of experiments, the tissues were Na^+ loaded by incubation in K^+-free (additional NaCl added instead of KCl) Ca^{2+}-free (no $CaCl_2$ plus 0.1 mM EGTA) solution, treated with 100-μM L-NAME and 30-μM cyclopiazonic acid (CPA) and then with or without 20-μM caloxin. Contraction was then monitored at specified Ca^{2+} concentrations.

Data analysis

For non-competitive inhibition in the presence of saturating substrates, v = Vmax/(1+[I]/Ki), here v is the reaction velocity obtained in the presence of the inhibitor concentration [I], Vmax is the velocity in the absence of the inhibitor and Ki is the inhibition constant. To compute values of Ki, for the non-competitive inhibition, the data were analyzed by non-linear regression according to the equation: percent inhibition = 100 $\times$ [inhibitor]/(Ki + [inhibitor]). Curve fitting was carried out using FigP software (Ancaster, Canada). It is also deduced that for the fractional inhibition f (Vmax – v)/Vmax (or percent inhibition if Vmax is taken to be 100), f + fKi/I =1. Hence a plot of f/I *versus* f would be linear with the slope of –1/Ki. The initial data were also analyzed by linear regression using this equation. In contractility experiments, the force of contraction for each tissue was expressed as percent of the force obtained in the second KCl contraction. Statistical significance was determined using one-way ANOVA and Tukey-Kramer Multiple Comparisons Test using the software GraphPad Instat (SanDiego, USA) or Student's t-test when only two groups were compared. Values of $P < 0.05$ were considered to be significant.

Results

Construction and screening of phage display library of caloxin 1b1-like peptides

We tested the hypothesis that altering 1, 2 or 3 residues in caloxin 1b1 may improve its affinity and isoform selectivity and yet maintain the ability to inhibit PMCA. Since we did not know which mutations would be most effective, we created a phage display library encoding caloxin 1b1-like peptides to screen for such peptides. The 12 amino acid sequence unique to caloxin 1b1 is TAWSEVLHLLSR [42]. We computed that an optimized library could be created to contain 76.1% phage-encoding peptides with 0, 1, 2, 3 or >3 amino acid substitutions as described in the Experimental Methods. The constructed M13 KE library of caloxin 1b1-like peptides had a diversity of 7×10^5 plaque-forming units (pfu). Sequencing 38 clones showed that there was no difference between the expected and the obtained frequencies of peptides with 0, 1, 2, 3 or >3 amino acid substitutions (Table 1).

The caloxin 1b1-like library was amplified once and then 2×10^8 pfu were used for screening by four rounds of affinity chromatography with PMCA purified from human erythrocyte ghosts. The titre decreased after each round and 315 pfu remained at the end. Of these, 105 clones were sequenced and they encoded 33 different peptides. Frequencies of clones encoding key peptides are in Table 2. We also considered that there may be a bias in the library construction and amplification. For example, the library would contain approximately 2,000 times more copies of caloxin 1b1 than that of a phage encoding a given single species of peptide with three amino acid substitutions. Amplification efficiencies of individual phage clones may also be different. Therefore, to further select the phage on their ability to bind PMCA4, we allowed an equal amount of each of the 33 clones (10^6 pfu total) to compete against each other for binding to PMCA4 in four rounds of affinity chromatography. This resulted in 450 pfu of which 48 clones were sequenced. Frequencies of the clones encoding key peptides are in Table 2. Three of the most frequent sequences in the final round after the competition were designated caloxin 1c1, 1c2 and 1c3. Probabilities of obtaining the observed frequencies purely by chance for the three peptides were less than 0.0005.

Inhibition of PMCA4 by caloxin 1b1 mutants

In the phage, the variable 12 amino acid sequence is followed by the amino acid sequence GGGSK and then the remainder of the gIII protein. Therefore, caloxins 1c1 (TTWSEVVHRLSRGGGSK-amide), 1c2 (TAWSEVLDLLRRGGGSK-amide) and 1c3 (ASWSEVLHLLSRGGGSK-amide) were synthesized. Difference in Mg^{2+}–ATPase activity in erythrocyte ghosts (express mainly PMCA4) with and without Ca^{2+} was defined as the PMCA Ca^{2+}–Mg^{2+}–ATPase [42]. The assay solution contained inhibitors of SERCA (thapsigargin), Na^+–K^+–ATPase (ouabain) and mitochondrial Ca^{2+}–ATPase (azide). As reported previously for caloxin 1b1, none of the peptides inhibited the ATP hydrolysis in the absence of Ca^{2+} [42]. Figure 1

Table 1 Characterization of caloxin 1b1-like library

Number of amino acid substitutions	Observed frequency	Expected frequency
0	5.3	10
1	23.7	25.6
2	28.9	29.7
3	23.7	20.8
>3	18.4	13.9

Note: The library was constructed with 91% of the original base and 3% of each of the other three in the caloxin 1b1-coding domain. A total of 38 clones were sequenced. The frequency values are given as percent of total. The chi-square value test showed that the distributions of the expected and the observed distributions are not significantly different ($P > 0.05$).

shows the effects of the parent peptide caloxin 1b1, its randomized control peptide RP1b1 and the three mutant peptides. The control peptide RP1b1 had no effect on the PMCA Ca^{2+}–Mg^{2+}–ATPase activity. We have previously shown that caloxin inhibition is non-competitive [50]. Therefore, the Ki values were determined at saturating substrate concentrations as described in the Methods. Using non-linear regression, the Ki values of the various caloxins were 1b1: 45 ± 4, 1c1: 20 ± 3, 1c2: 2.3 ± 0.3 and 1c3: 18 ± 3 μM. Analysis of the same data by linear regression as described in the Methods gave Ki values similar to those using non-linear regression: 1b1: 55 ± 14, 1c1: 12 ± 3, 1c2: 2.0 ± 0.1 and 1c3: 20 ± 6 μM. In all subsequent experiments, only the non-linear regression was used. Thus, the selected caloxin 1b1-like mutants inhibited the erythrocyte ghost Ca^{2+}–Mg^{2+}–ATPase with greater affinity than that of the parent caloxin 1b1. Caloxin 1c2 had the highest affinity with its Ki value (2.3 ± 0.3 μM) being one-twentieth that of caloxin 1b1 (45 ± 4 μM).

Inhibition of different PMCA isoforms by caloxin 1c2

Caloxin 1c2 was obtained by mutagenesis of caloxin 1b1, which had been selected with the extracellular domain 1a of PMCA4 (residues 115–131) as a target. However, sequences of the extracellular domain 1a between PMCA genes contain several similar residues but are not identical (Fig. 2A). Therefore, we compared the effects of caloxins 1b1 and 1c2 on the Ca^{2+}–Mg^{2+}–ATPase activities of PMCA1–4 (Fig. 2B and Fig. 2C). The values of Ki in μM for caloxin 1b1 were PMCA1 (105 ± 11), PMCA2 (167 ± 67), PMCA3 (274 ± 40) and PMCA4 (45 ± 4). Thus caloxin 1b1 inhibited PMCA4 with slightly higher affinity than for PMCA1, 2 or 3. In contrast, caloxin 1c2 had much

Table 2 Percent frequencies of key sequences obtained during screening

Sequence	Initial screening	After competition
TTWSEVVHRLSR - caloxin 1c1	0.9	35.4
TAWSEVLDLLRR - caloxin 1c2	24.6	16.7
ASWSEVLHLLSR - caloxin 1c3	9.5	14.6
TAWSEVLHLLSR - caloxin 1b1	20.8	0
ASWSDVLHLLSR	7.6	4.1
TGWSEVLHLLSR	4.8	6.2
TAWSDVLHLLSR	3.8	0

Note: A total of 105 clones were sequenced at the end of the initial four rounds of screening, and 48 clones were sequenced at the end of the four rounds of competition. The frequency values are given as percent of the number of clones sequenced at each step.

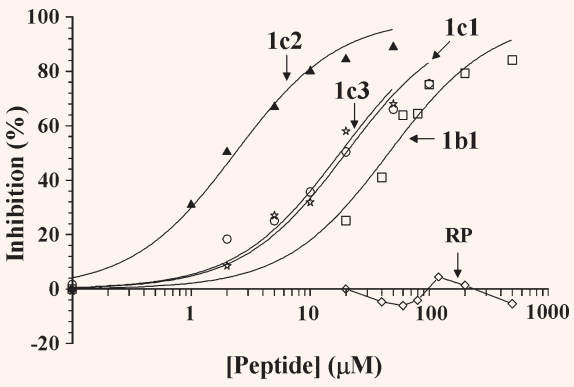

Fig. 1 Inhibition of Ca^{2+}–Mg^{2+}–ATPase in human erythrocyte ghosts at different concentrations of caloxin 1b1 and its mutants 1c1, 1c2, 1c3. Each value is the mean from 3–4 measurements carried out on 2–4 different days. On each day, the mean value of the Ca^{2+}–Mg^{2+}–ATPase was taken as 100% to compute the percent inhibition.

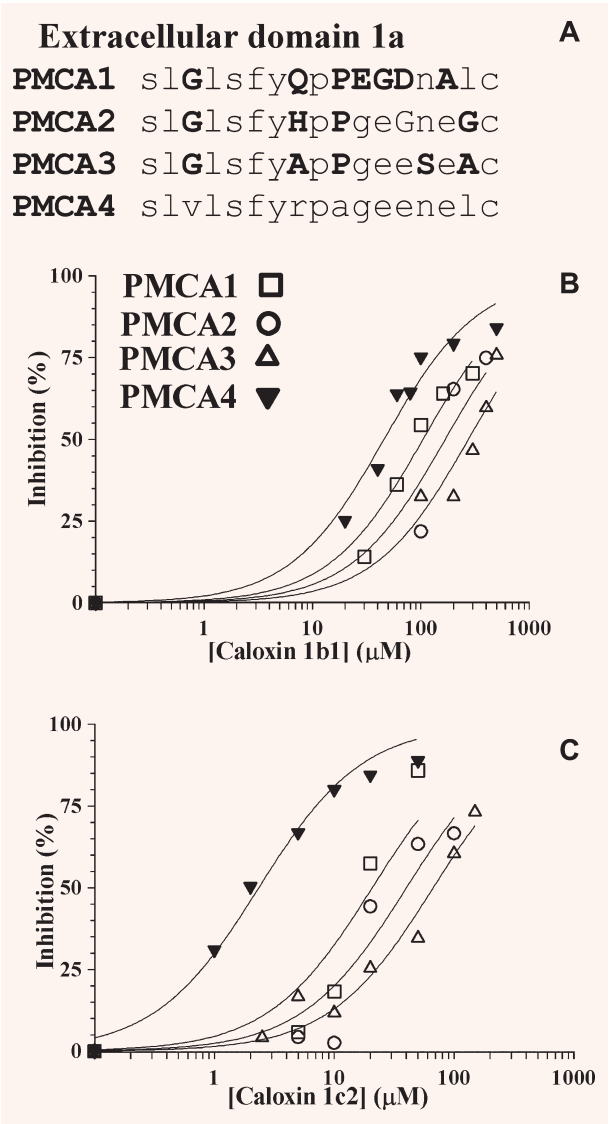

Fig. 2 Inhibition of PMCA1, 2, 3 and 4 Ca^{2+}–Mg^{2+}–ATPases by caloxins 1b1 (**B**) and 1c2 (**C**). Sequences of the extracellular domain 1a of PMCA4 that was used as synthetic target for screening are also compared with the domains 1a of PMCA1, 2 and 3 (**A**). Rabbit duodenal muscosal PM rich fraction was used as source of PMCA1, human erythrocyte ghosts as source of PMCA4 and microsomes from overexpressing insect cells sf9 for PMCA2 and 3. Each value is mean from 3–4 measurements carried out on 2–4 different days. On each day, the mean value of the Ca^{2+}–Mg^{2+}–ATPase was taken as 100% to compute the percent inhibition.

greater selectivity for PMCA4: Ki in μM for caloxin 1c2 were: PMCA1 (21 ± 6), PMCA2 (40 ± 10), PMCA3 (67 ± 8) and PMCA4 (2.3 ± 0.3). Thus, when

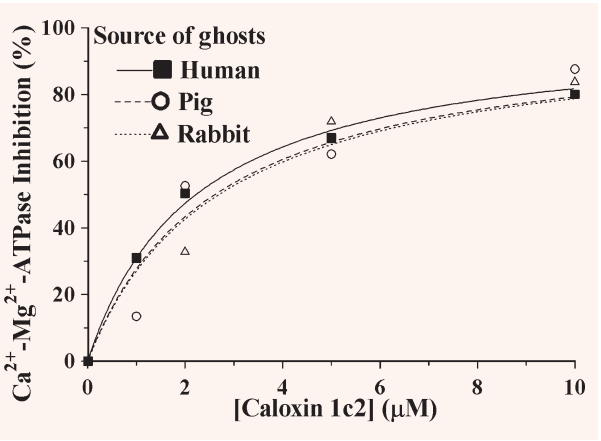

Fig. 3 Caloxin 1c2 inhibition of PMCA Ca^{2+}–Mg^{2+}–ATPase in erythrocyte ghosts from different species.

compared to caloxin 1b1, caloxin 1c2 had a much greater affinity and higher selectivity for PMCA4.

Caloxin 1c2 inhibition of PMCA in erythrocyte ghosts of different species

The sequence of the extracellular domain 1 differs slightly between human, pig and rabbit. Therefore, we tested the inhibition of PMCA Ca^{2+}–Mg^{2+}–ATPase in the erythrocyte ghosts from these species (Fig. 3). Caloxin 1c2 inhibited the Ca^{2+}–Mg^{2+}–ATPase with similar Ki values (in μM) in erythrocyte ghosts from human (2.3 ± 0.3), pig (2.6 ± 0.6) and rabbit (2.73 ± 0.5) ($P > 0.05$). Thus, caloxin 1c2 can be used for experiments in various species.

Roles of different residues in 1c2

The first two and the last five residues vary between caloxins 1b1, 1c1, 1c2 and 1c3 (Table 2). Caloxin 1b1 contained WSEVL at residues 3–7. This sequence or its conservative substitutions WS(E/D)V(L/V) appeared at this location in 88% of the clones in the initial screening and in 96% of the clones after the competition. Caloxins 1b1, 1c1, 1c2 and 1c3 all contained the moiety WS(E/D)V(L/V). The residue W was present in position 3 in sequences of 95% of the clones obtained after the first rounds of screening and 100% of those after the competition.

The residue benzoylphenylalanine (Bpa) has been used in the literature as a conservative change for W

[51, 52]. To further investigate the role of the moiety WS(E/D)V(L/V) and that of the C-terminal end added to the variable sequence (TAWSEVLDLLRR) of 1c2, we synthesized two additional peptides:

3Bpa1c2biotin (TA[Bpa]SEVLDLLRRGGGSK (biotin)-amide) and 16Bpa1c2biotin (TAWSEVLDLL-RRGGG[Bpa]K[biotin]-amide). If the C-terminal domain were to play a role in the inhibition, the 16Bpa substitution and the change in the positive charge of K at 17 by adding biotin to the epsilon amino group would result in weaker inhibition by the 16Bpa1c2biotin. However, if the moiety WS(E/D)-V(L/V) were to be key to the inhibition, 3Bpa1c2biotin would be a weak inhibitor. The effects of both the derivatives were examined on the human erythrocyte ghost Ca^{2+}–Mg^{2+}–ATPase as the Ca^{2+}-stimulated hydrolysis of [^{33}P]-γ-ATP (Fig. 4). The Ki value for 16Bpa1c2biotin derivative (5.1 ± 0.8 μM) was only slightly greater than that of caloxin 1c2 (2.3 ± 0.3 μM). Thus the substitution of 16S with Bpa and biotinylation of K altered the PMCA inhibition only marginally, consistent with these residues being outside the selected 12 amino acid domain of caloxin 1c2. In contrast, the Ki value for the 3Bpa1c2biotin (50 ± 6 μM) was much greater. This experiment confirmed the hypothesis that the moiety WS(E/D)-V(L/V) in caloxin 1b1 and its mutants is important in inhibiting PMCA4 Ca^{2+}–Mg^{2+}–ATPase. This observation may be useful in further studies on caloxin 1c2-membrane interactions.

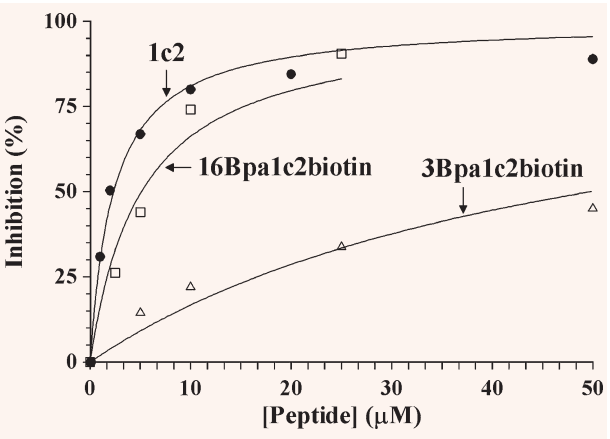

Fig. 4 Inhibition of PMCA Ca^{2+}–Mg^{2+}–ATPase in human erythrocyte ghosts by caloxin 1c2 derivatives.

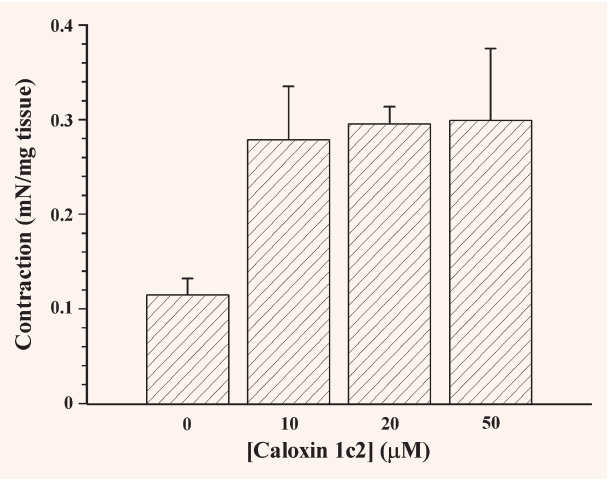

Fig. 5 Effect of caloxin 1c2 on basal tone of coronary artery. De-endothelialized coronary artery rings were contracted in 60 mM KCl, washed in Krebs' solution and incubated in this solution containing 100 μM L-NAME for 1 hr and then 0, 10, 20 or 50 μM caloxin 1c2 was added. An increase in contraction in 20 min after addition of the caloxin 1c2 was determined as mN/mg tissue weight. The values are mean ± SEM of 18, 12, 7 and 7 replicates for 0, 10, 20 or 50 μM caloxin 1c2, respectively.

Effects of caloxin 1c2 on coronary artery smooth muscle contractility

We next examined the effects of 0, 10, 20 and 50 μM caloxin 1c2 on basal tone of de-endothelialized coronary artery [42, 49, 53]. The final ethanol concentration in all the four groups was 0.01%. Time course of the tone development was examined (data not shown). There was no significant effect of caloxin 1c2 within 2 min. Only 20 and 50 μM caloxin 1c2 gave an increase after 5 min, whereas 10 μM caloxin 1c2 also gave a significant increase after 10 min. At all the three caloxin 1c2 concentrations, the caloxin induced increase in basal tone leveled off after 20 min at 2–3 % of the maximum response obtained with 60 mM KCl (Fig. 5). A multiple comparison test using one way-ANOVA negated the hypothesis that the differences in contraction in 0, 10, 20 and 50 μM caloxin 1c2 were purely due to chance ($P = 0.0015$). In a Tukey–Kramer multiple comparison test, q values of greater than 3.807 would indicate that a group differed from another comparison group. In this test there was significant difference between control tissues and those challenged with 10 ($q = 4.085$, $P < 0.05$), 20 ($q = 5.235$,

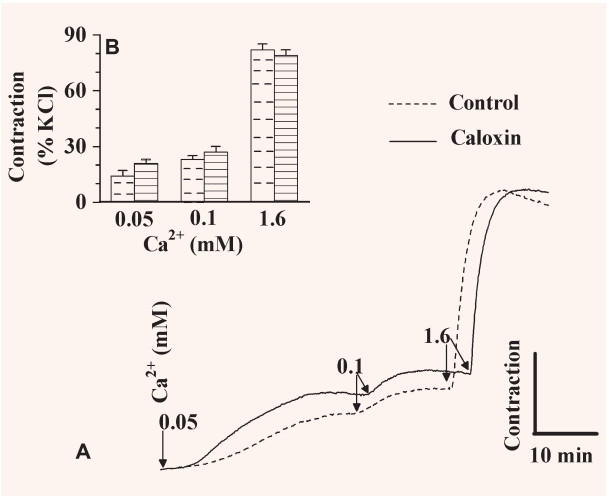

Fig. 6 Effect of caloxin 1c2 on contraction of Na^+-loaded coronary artery smooth muscle. (**A**) Representative tracings. De-endothelialized coronary artery rings were contracted in 60 mM KCl, washed in Krebs' solution and then Na^+-loaded by incubation in K^+-free Ca^{2+}-free solution for 45 min and then 100 μM L-NAME and 30 μM CPA were added and after another 45 min 20 μM caloxin 1c2 was added to some tissues and equal amount of ethanol to the control tissues. After another 15 min, $CaCl_2$ was added to obtain the specified concentrations of free Ca^{2+} compensating for the EGTA present previously. Contraction of each artery was expressed as percent of that obtained with 60 mM KCl. The contraction bar indicates a force of contraction 20% of that obtained with 60 mM KCl. (**B**) A histogram comparing the force of contraction obtained at 50, 100 and 1600 μM Ca^{2+}. The values are mean ± SEM of 11 replicates.

$P < 0.05$) and 50 (q = 4.156, $P < 0.05$) μM caloxin 1c2. Furthermore, there was no significant difference between tissues treated with 10 or 20 (q = 1.435, $P > 0.05$), 10 or 50 (q = 0.7679, $P > 0.05$) and 20 or 50 (q = 0.5133, $P > 0.05$) μM caloxin 1c2.

We also examined the effect of caloxin 1c2 on de-endothelialized coronary artery rings, which were Na^+-loaded and SERCA was inhibited with CPA. Incubating smooth muscle in K^+-free Krebs' solution Na^+ loads the smooth muscle tissues that contract in presence of Ca^{2+} [49, 54]. Depending on the Na^+ and Ca^{2+} electrochemical gradients, NCX can operate in forward mode (Ca^{2+} extrusion) or in reverse mode (Ca^{2+} entry). In the Na^+-loaded cells, NCX would only allow Ca^{2+} entry into the cell but not Ca^{2+} extrusion. Thus, PMCA would be the only system that could lower cytosolic Ca^{2+} levels. We incubated the tissues in K^+-free and Ca^{2+}-free Krebs' solution, and added CPA to inhibit SERCA. The force of contraction increased in all the tissues when Ca^{2+} concentration in the medium was increased. However, at 0.05 mM extracellular Ca^{2+}, tissues in caloxin 1c2 showed significantly greater force of contraction (P = 0.019) than the control tissues (Fig. 6). Caloxin 1c2 did not affect the force of contraction at 0.1 (P = 0.2267) and 1.6 (P = 0.4717) mM extracellular Ca^{2+}. Thus, caloxin 1c2 increased Ca^{2+} sensitivity of the tissues when they were Na^+-loaded and SERCA was inhibited. However, the maximum force of contraction was not altered.

Discussion

The Results show that creating and screening a caloxin 1b1-like library yielded the mutant 1c2 with a greater affinity for PMCA and selectivity for PMCA4 over other PMCA isoforms. An analysis of structural features of caloxin 1c2 is presented. Finally, caloxin 1c2 affects coronary contractility. Discussion will focus on the methods used, interpretation of the results and potential utility of the PMCA4 selective caloxin.

The first reported caloxin was 2a1. It had a Ki of >500 μM and has proved useful in studies on PMCA in various tissues [11,55–57]. Caloxin 1b1 was obtained by an improved screening procedure and had a 10× higher affinity than caloxin 2a1 and it was slightly selective for PMCA4 [42]. Here, the key concept in the use of the caloxin 1b1-like library was that limited mutagenesis could be used to select peptides that retain the ability to inhibit PMCA but have greater affinity and isoform selectivity than the parent peptide. This concept was validated by obtaining caloxin 1c2 by screening a phage display library of caloxin 1b1-like peptides. Caloxin 1c2 has a 200x and 20x higher affinity than caloxins 2a1 and 1b1, respectively. Even though phage display was used in this work, the concepts and methods developed here would be equally applicable to other screening methods. The algorithm was written for a specific peptide of 12 amino acid residues but it can be used for any peptides, which are 12 amino acids long or shorter. The code for the Macro written in Microsoft Office Excel can be obtained by writing to the authors.

We have previously proposed that due to low capacity, small co-operativity to Ca^{2+}, low Km for

$MgATP^{2-}$, broad pH profile and less sensitivity to reactive oxygen, PMCA may be important in intracellular Ca^{2+} homeostasis [58]. However, coronary artery smooth muscle expresses PMCA4 and PMCA1 [26, 42]. However, it is not clear if they both play a similar role in Ca^{2+} homeostasis. The Ki values of caloxin 1c2 are 2.3 ± 0.3 μM for PMCA4 and 21 ± 6 μM for PMCA1. Thus, at 10 μM it would inhibit mainly PMCA4 and at 50 μM it would inhibit both. A slight increase in tone observed with caloxin 1c2 is consistent with the role of PMCA in Ca^{2+} homeostasis. The caloxin-induced increase in tone developed slower at 10 μM caloxin 1c2 than at the higher concentrations suggesting a slow diffusion of this large molecule (approximately 2 kD) in the tissue. The small effect of caloxin 1c2 on the tone is unlikely to be due to proteolysis since after 20 min, different concentrations (10, 20 or 50 μM) of caloxin 1c2 caused a similar increase. These data suggest that PMCA4 is involved in the control of basal tone. However, this result needs to be confirmed using a PMCA1 selective caloxin, which is yet to be invented.

We also examined the effects of caloxin 1c2 in Na^+-loaded tissues in presence of CPA. The idea was to determine the role of PMCA in Ca^{2+} extrusion under the conditions in which SERCA pump and NCX-mediated Ca^{2+} extrusion are inhibited. There are no selective inhibitors for NCX-mediated Ca^{2+} extrusion that can be added extracellularly. Amiloride derivatives and KB-R7943 have multiple effects, SEA 0400 can inhibit only NCX-mediated Ca^{2+} entry and XIP acts cytoplasmically and does not enter the cells when added extracellularly [59]. In tissues containing low extracellular Na^+ or high intracellular Na^+, the NCX-mediated Ca^{2+} entry occurs but not the NCX-mediated Ca^{2+} extrusion. However, intracellular acidosis occurs when coronary artery smooth muscle cells are placed in solution containing low extracellular Na^+ [60]. Therefore, we examined the effects of caloxin 1c2 in Na^+-loaded tissues in presence of CPA. The results showed that caloxin 1c2 increased the contraction at 0.05 mM extracellular Ca^{2+} but not at 0.1 and 1.6 mM. These results are consistent with the role of PMCA in Ca^{2+} extrusion and also with PMCA being a low capacity Ca^{2+} extrusion system.

Caloxin 1c2 is a novel inhibitor, which is selective for PMCA4 over PMCA1, 2 and 3. Using this inhibitor we have reported the role of PMCA4 in coronary artery contractility. This work, however, presents further questions concerning the roles of PMCA4 in nNOS activation and interactions between SERCA and NCX and PMCA. Furthermore, large and small coronary arteries show different responses to various agents and their SERCA content [61, 62]. Caloxin 1c2 provides a tool to dissect the role of PMCA4 in these tissues. Caloxin 1c2 may also provide a tool to examine the roles of PMCA4 present in different cell types and/or in specific organelles such as lipid rafts or caveolae. Based on work with transgenic mice, PMCA4 plays a role in sperm motility [32]. Caloxin 1c2 would allow a further examination of this issue.

Abbreviations

Bpa, benzoyl phenylalanine; caloxin, a substance that binds the PM Ca^{2+} pump on its external surface and modulates its activity; $[Ca^{2+}]i$, cytosolic $[Ca^{2+}]$; CPA, cyclopiazonic acid; EDTA, ethylenediamine tetra-acetic acid; EGTA, ethylene glycol-bis(β-aminoethyl ether)-N,N,N,'N,'-tetraacetic acid; HEPES, N-2-hydroxyethylpiperazine-N'-2-ethanesulfonic acid; L-NAME, L-nitroarginylmethyl ester; NCX, Na^+-Ca^{2+}-exchanger; PM, plasma membrane; PMCA, PM Ca^{2+} pump; NO, nitric oxide; pfu, plaque forming units; SERCA, sarco/endoplasmic reticulum Ca^{2+} pump.

Acknowledgements

Microsomes enriched in PMCA2 and PMCA3 were a gift from Dr. A. Filoteo of Mayo Clinic College of Medicine (Rochester, Minnesota). We thank Sue E. Samson, Mythili Pathmanathan and Fareeha Qayyum for assisting in this work, and Dr. P. K. Rangachari for his suggestions. This work was supported by grant NA5783 from the Heart & Stroke Foundation of Ontario.

References

1. **Carafoli E.** Calcium signaling: a tale for all seasons. *Proc Natl Acad Sci.USA* 2002; 99: 1115–22.
2. **Dode L, Vilsen B, Van Baelen K, Wuytack F, Clausen JD, Andersen JP.** Dissection of the functional differences between sarco(endo)plasmic retic-

ulum Ca^{2+}-ATPase (SERCA) 1 and 3 isoforms by steady-state and transient kinetic analyses. *J Biol Chem.* 2002; 277: 45579–91.

3. **Frieden M, Malli R, Samardzija M, Demaurex N, Graier WF.** Subplasmalemmal endoplasmic reticulum controls K(Ca) channel activity upon stimulation with a moderate histamine concentration in a human umbilical vein endothelial cell line. *J Physiol.* 2002; 540: 73–84.
4. **Philipson KD, Nicoll DA, Ottolia M, Quednau BD, Reuter H, John S, Qiu Z.** The Na^+/Ca^{2+} exchange molecule: an overview. *Ann N Y Acad Sci.* 2002; 976: 1–10.
5. **Pande J, Grover AK.** Plasma membrane calcium pumps in smooth muscle: from fictional molecules to novel inhibitors. *Can J Physiol Pharmacol.* 2005; 83: 743–54.
6. **Strehler EE, Treiman M.** Calcium pumps of plasma membrane and cell interior. *Curr Mol Med.* 2004; 4: 323–35.
7. **Shull GE, Okunade G, Liu LH, Kozel P, Periasamy M, Lorenz JN, Prasad V.** Physiological functions of plasma membrane and intracellular Ca^{2+} pumps revealed by analysis of null mutants. *Ann N Y Acad Sci.* 2003; 986: 453–60.
8. **Wuytack F, Raeymaekers L, Missiaen L.** Molecular physiology of the SERCA and SPCA pumps. *Cell Calcium.* 2002; 32: 279–305.
9. **Stauffer TP, Guerini D, Carafoli E.** Tissue distribution of the four gene products of the plasma membrane Ca^{2+} pump. A study using specific antibodies. *J Biol Chem.* 1995; 270: 12184–90.
10. **Strehler EE, Caride AJ, Filoteo AG, Xiong Y, Penniston JT, Enyedi A.** Plasma membrane Ca^{2+} ATPases as dynamic regulators of cellular calcium handling. *Ann N Y Acad Sci.* 2007; 1099: 226–36.
11. **van Breemen C, Chen Q, Laher I.** Superficial buffer barrier function of smooth muscle sarcoplasmic reticulum. *Trends Pharmacol Sci.* 1995; 16: 98–105.
12. **Barr SC, Pannabecker TL, Gilmour RF, Jr., Chandler JS.** Upregulation of cardiac cell plasma membrane calcium pump in a canine model of Chagas disease. *J Parasitol.* 2003; 89: 381–4.
13. **Husain M, Jiang L, See V, Bein K, Simons M, Alper SL, Rosenberg RD.** Regulation of vascular smooth muscle cell proliferation by plasma membrane $Ca(^{2+})$-ATPase. *Am J Physiol.* 1997; 272: C1947–C59.
14. **Lehotsky J, Kaplan P, Murin R, Raeymaekers L.** The role of plasma membrane Ca^{2+} pumps (PMCAs) in pathologies of mammalian cells. *Front Biosci.* 2002; 7: d53–84.
15. **Oceandy D, Buch MH, Cartwright EJ, Neyses L.** The emergence of plasma membrane calcium pump as a novel therapeutic target for heart disease. *Mini Rev Med Chem.* 2006; 6: 583–8.
16. **Burette A, Rockwood JM, Strehler EE, Weinberg RJ.** Isoform-specific distribution of the plasma membrane Ca^{2+} ATPase in the rat brain. *J Comp Neurol.* 2003; 467: 464–76.
17. **Brini M, Coletto L, Pierobon N, Kraev N, Guerini D, Carafoli E.** A comparative functional analysis of plasma membrane Ca^{2+} pump isoforms in intact cells. *J Biol Chem.* 2003; 278: 24500–8.
18. **Caride AJ, Penheiter AR, Filoteo AG, Bajzer Z, Enyedi A, Penniston JT.** The plasma membrane calcium pump displays memory of past calcium spikes. Differences between isoforms 2b and 4b. *J Biol Chem.* 2001; 276: 39797–804.
19. **Caride AJ, Filoteo AG, Enyedi A, Verma AK, Penniston JT.** Detection of isoform 4 of the plasma membrane calcium pump in human tissues by using isoform-specific monoclonal antibodies. *Biochem J.* 1996; 316: 353–9.
20. **Filoteo AG, Elwess NL, Enyedi A, Caride A, Aung HH, Penniston JT.** Plasma membrane Ca^{2+} pump in rat brain. Patterns of alternative splices seen by isoform-specific antibodies. *J Biol Chem.* 1997; 272: 23741–7.
21. **Howard A, Barley NF, Legon S, Walters JR.** Plasma-membrane calcium-pump isoforms in human and rat liver. *Biochem J.* 1994; 303: 275–9.
22. **Guerini D.** The significance of the isoforms of plasma membrane calcium ATPase. *Cell Tissue Res.* 1998; 292: 191–7.
23. **Krizaj D, Demarco SJ, Johnson J, Strehler EE, Copenhagen DR.** Cell-specific expression of plasma membrane calcium ATPase isoforms in retinal neurons. *J Comp Neurol.* 2002; 451: 1–21.
24. **Caride AJ, Filoteo AG, Penniston JT, Strehler EE.** The plasma membrane Ca^{2+} pump isoform 4a differs from isoform 4b in the mechanism of calmodulin binding and activation kinetics. Implications for Ca^{2+} signaling. *J Biol Chem.* 2007; 282: 25640–8.
25. **Talarico EF Jr, Kennedy BG, Marfurt CF, Loeffler KU, Mangini NJ.** Expression and immunolocalization of plasma membrane calcium ATPase isoforms in human corneal epithelium. *Mol Vis.* 2005; 11: 169–78.
26. **Szewczyk MM, Davis KA, Samson SE, Simpson F, Rangachari PK, Grover AK.** Ca^{2+}-pumps and Na^{2+}-Ca^{2+}-exchangers in coronary artery endothelium *versus* smooth muscle. *J Cell Mol Med.* 2007; 11: 129–38.
27. **Amino K, Honda Y, Ide C, Fujimoto T.** Distribution of plasmalemmal Ca(2+)-pump and caveolin in the corneal epithelium during the wound healing process. *Curr Eye Res.* 1997; 16: 1088–95.

28. **Kip SN, Strehler EE.** Rapid downregulation of NCX and PMCA in hippocampal neurons following H2O2 oxidative stress. *Ann NY Acad Sci.* 2007; 1099: 436–39.
29. **Ishida Y, Paul RJ.** Ca^{2+} clearance in smooth muscle: lessons from gene-altered mice. *J Smooth Muscle Res.* 2005; 41: 235–45.
30. **Kao J, Fortner CN, Liu LH, Shull GE, Paul RJ.** Ablation of the SERCA3 gene alters epithelium-dependent relaxation in mouse tracheal smooth muscle. *Am J Physiol.* 1999; 277: L264–70.
31. **Liu L, Ishida Y, Okunade G, Pyne-Geithman GJ, Shull GE, Paul RJ.** Distinct roles of PMCA isoforms in Ca^{2+} homeostasis of bladder smooth muscle: evidence from PMCA gene-ablated mice. *Am J Physiol Cell Physiol.* 2007; 292: C423–31.
32. **Okunade GW, Miller ML, Pyne GJ, Sutliff RL, O'Connor KT, Neumann JC, Andringa A, Miller DA, Prasad V, Doetschman T, Paul RJ, Shull GE.** Targeted ablation of plasma membrane Ca2+-ATPase (PMCA) 1 and 4 indicates a major housekeeping function for PMCA1 and a critical role in hyperactivated sperm motility and male fertility for PMCA4. *J Biol Chem.* 2004; 279: 33742–50.
33. **Prasad V, Okunade GW, Miller ML, Shull GE.** Phenotypes of SERCA and PMCA knockout mice. *Biochem Biophys Res Commun.* 2004; 322: 1192–203.
34. **Prasad V, Okunade G, Liu L, Paul RJ, Shull GE.** Distinct phenotypes among plasma membrane Ca2+-ATPase knockout mice. *Ann NY Acad Sci.* 2007; 1099: 276–86.
35. **Gros R, Afroze T, You XM, Kabir G, Van Wert R, Kalair W, Hoque AE, Mungrue IN, Husain M.** Plasma membrane calcium ATPase overexpression in arterial smooth muscle increases vasomotor responsiveness and blood pressure. *Circ Res.* 2003; 93: 614–21.
36. **Schuh K, Quaschning T, Knauer S, Hu K, Kocak S, Roethlein N, Neyses L.** Regulation of vascular tone in animals overexpressing the sarcolemmal calcium pump. *J Biol Chem.* 2003; 278: 41246–52.
37. **Strehler EE, Zacharias DA.** Role of alternative splicing in generating isoform diversity among plasma membrane calcium pumps. *Physiol Rev.* 2001; 81: 21–50.
38. **Hammes A, Oberdorf-Maass S, Rother T, Nething K, Gollnick F, Linz KW, Meyer R, Hu K, Han H, Gaudron P, Ertl G, Hoffmann S, Ganten U, Vetter R, Schuh K, Benkwitz C, Zimmer HG, Neyses L.** Overexpression of the sarcolemmal calcium pump in the myocardium of transgenic rats. *Circ Res.* 1998; 83: 877–88.
39. **Daniel EE, El Yazbi A, Cho WJ.** Caveolae and calcium handling, a review and a hypothesis. *J Cell Mol Med.* 2006; 10: 529–44.
40. **Fujimoto T.** Calcium pump of the plasma membrane is localized in caveolae. *J Cell Biol.* 1993; 120: 1147–57.
41. **Sepulveda MR, Berrocal-Carrillo M, Gasset M, Mata AM.** The plasma membrane Ca^{2+}-ATPase isoform 4 is localized in lipid rafts of cerebellum synaptic plasma membranes. *J Biol Chem.* 2006; 281: 447–53.
42. **Pande J, Mallhi KK, Sawh A, Szewczyk MM, Simpson F, Grover AK.** Aortic smooth muscle and endothelial plasma membrane Ca^{2+} pump isoforms are inhibited differently by the extracellular inhibitor caloxin 1b1. *Am J Physiol Cell Physiol.* 2006; 290: C1341–9.
43. **Chaudhary J, Walia M, Matharu J, Escher E, Grover AK.** Caloxin: a novel plasma membrane Ca^{2+} pump inhibitor. *Am J Physiol Cell Physiol.* 2001; 280: C1027–30.
44. **Niggli V, Zurini M, Carafoli E.** Purification, reconstitution, and molecular characterization of the Ca^{2+} pump of plasma membranes. *Methods Enzymol.* 1987; 139: 791–808.
45. **Grover AK, Samson SE, Lee RM.** Subcellular fractionation of pig coronary artery smooth muscle. *Biochim Biophys Acta* 1985; 818: 191–9.
46. **Narayanan N, Su N, Bedard P.** Inhibitory and stimulatory effects of fluoride on the calcium pump of cardiac sarcoplasmic reticulum. *Biochim Biophys Acta* 1991; 1070: 83–91.
47. **Pande J, Mallhi KK, Grover AK.** A novel plasma membrane Ca^{2+}-pump inhibitor: caloxin 1A1. *Eur J Pharmacol.* 2005; 508: 1–6.
48. **Carafoli E.** The Ca^{2+} pump of the plasma membrane. *J Biol Chem* 1992; 267: 2115–8.
49. **Elmoselhi A, Butcher A, Samson SE, Grover AK.** Coronary artery contractility, Na(+)-pump and oxygen radicals. *Gen Physiol Biophys.* 1994; 13: 247–56.
50. **Holmes ME, Chaudhary J, Grover AK.** Mechanism of action of the novel plasma membrane Ca(2+)-pump inhibitor caloxin. *Cell Calcium.* 2003; 33: 241–5.
51. **Cuppoletti J, Malinowska DH.** Interaction of polypeptides with the gastric ($H^+ + K^+$)ATPase: melittin, synthetic analogs, and a potential intracellular regulatory protein. *Mol Cell Biochem.* 1992; 114: 57–63.
52. **Kauer JC, Erickson-Viitanen S, Wolfe HR Jr, DeGrado WF.** p-Benzoyl-L-phenylalanine, a new photoreactive amino acid. Photolabeling of calmodulin with a synthetic calmodulin-binding peptide. *J Biol Chem.* 1986; 261: 10695–700.

53. **Grover AK, Samson SE.** Peroxide resistance of ER Ca^{2+} pump in endothelium: implications to coronary artery function. *Am J Physiol.* 1997; 273: C1250–8.
54. **Taylor GS, Paton DM, Daniel EE.** Characteristics of electrogenic sodium pumping in rat myometrium. *J Gen Physiol.* 1970; 56: 360–75.
55. **De Luisi A, Hofer AM.** Evidence that Ca(2+) cycling by the plasma membrane Ca(2+)-ATPase increases the 'excitability' of the extracellular Ca(2+)-sensing receptor. *J Cell Sci.* 2003; 116: 1527–38.
56. **Kawano S, Otsu K, Shoji S, Yamagata K, Hiraoka M.** Ca(2+) oscillations regulated by Na(+)-Ca(2+) exchanger and plasma membrane Ca(2+) pump induce fluctuations of membrane currents and potentials in human mesenchymal stem cells. *Cell Calcium.* 2003; 34: 145–56.
57. **Vale-Gonzalez C, Gomez-Limia B, Vieytes MR, Botana LM.** Effects of the marine phycotoxin palytoxin on neuronal pH in primary cultures of cerebellar granule cells. *J Neurosci Res.* 2007; 85: 90–8.
58. **Grover AK, Samson SE.** Pig coronary artery smooth muscle: substrate and pH dependence of the two calcium pumps. *Am J Physiol.* 1986; 251: C529–34.
59. **Iwamoto T.** Forefront of Na^{+}/Ca^{2+} exchanger studies: molecular pharmacology of Na^{+}/Ca^{2+} exchange inhibitors. *J Pharmacol Sci.* 2004; 96: 27–32.
60. **Holmes ME, Mwanjewe J, Samson SE, Haist JV, Wilson JX, Dixon SJ, Karmazyn M, Grover AK.** Dehydroascorbic acid uptake by coronary artery smooth muscle: effect of intracellular acidification. *Biochem J.* 2002; 362: 507–12.
61. **Grover AK, Samson SE, Misquitta CM, Elmoselhi AB.** Effects of peroxide on contractility of coronary artery rings of different sizes. *Mol Cell Biochem.* 1999; 194: 159–64.
62. **Misquitta CM, Samson SE, Grover AK.** Sarcoplasmic reticulum Ca(2+)-pump density is higher in distal than in proximal segments of porcine left coronary artery. *Mol Cell Biochem.* 1996; 158: 91–5.